OPEN

Citation: Cell Death and Disease (2018) 8, e3178; doi:10.1038/cddis.2017.367
Official journal of the Cell Death Differentiation Association

www.nature.com/cddis

Influence of c-Src on hypoxic resistance to paclitaxel in human ovarian cancer cells and reversal of FV-429

Qinglong Guo[1,4], Lu Lu[1,4], Yan Liao[1], Xiaoping Wang[1], Yi Zhang[1], Yicheng Liu[1], Shaoliang Huang[1], Haopeng Sun[2], Zhiyu Li[3] and Li Zhao*[,1]

SRC family kinase was documented to have vital roles in adjusting cancer cell malignant behaviors. To date, the role of c-Src, a member of SRC family kinase, in resistance to paclitaxel in human ovarian cancer cells under hypoxia has not been investigated. In the present study, we discovered that hypoxic environment suppressed paclitaxel-induced G2/M phase arrest and blockade of c-Src improved ovarian cancer cells' sensitivity to paclitaxel. FV-429, a derivative of natural flavonoid wogonin, could suppress gene expression and activation of c-Src, followed by deteriorated Stat3 nuclear translocation and its binding to HIF-1α, resulting in paclitaxel resistance reversal through G2/M arrest potentiation. Our study demonstrated that c-Src contributed to hypoxic microenvironment-rendered paclitaxel resistance in human epithelial ovarian cancer cells by G2/M phase arrest deterioration, and through c-Src suppression, FV-429 was capable of reversing the resistance by blocking c-Src/Stat3/HIF-1α pathway.
Cell Death and Disease (2018) **8,** e3178; doi:10.1038/cddis.2017.367; published online 11 January 2018

In solid tumor, cells in hypoxic region becomes resistant to chemotherapy and radiotherapy, the reason for which is that hypoxia helps cancer cells survive by inducing several genes involved that accelerate the progression of malignancy.[1] Physiological hypoxia occurs when the oxygen tension falls below 2%, thus a cultivating environment containing 1% oxygen is commonly used to mimic hypoxic environment *in vitro*.[2–5] Ovarian cancer is a common gynecological cancer and one of the lethal cause of death from gynecological malignancy;[6] however, failure or relapse always exists due to the emergence of constant resistance. It has been reported that around 69% ovarian tumors from patients overexpress hypoxia inducible factor-1α (HIF-1α),[7,8] indicating that hypoxia may be closely related to ovarian tumors. Study showed that hypoxia increased G0/G1 phase percentage in ovarian cancer cells.[9] However, the effect of paclitaxel is based on the inhibition of microtubule depolymerization, leading to G2/M phase arrest in cancer cells, which can be weakened by the effect induced by hypoxia. Considering on the uncertainty, the resistance to paclitaxel is probably due to G1 phase promotion rendered by hypoxic environment. However, the inner mechanism of the regulation on this cell cycle arrest still remains unclear.

Non-receptor tyrosine kinase c-Src seems to be associated with hypoxia.[1,10–12] Signal transducer and activator of transcription 3 (Stat3), a transcription factor having vital roles in malignancy, can be activated by c-Src.[13] Mccann *et al.*[14] found that Stat3 activation contributed to hypoxia-induced resistance. Moreover, Huang *et al.*[9] found that blocking HIF-1α can improve G2/M arrest induced by paclitaxel under hypoxia. Thus we supposed that c-Src/Stat3/HIF-1α axis may regulate hypoxic resistance to paclitaxel under hypoxia.

FV-429, a derivative of wogonin, which is one of the main components extracted from *Scutellaria baicalensis Georgi*, exerted various anticancer activities.[15] It was optimized with bis (2-hydrocyethyl) amino propoxy substitution at C_7 position based on wogonin.[16] FV-429 has been reported to induce apoptosis of HepG2, MDA-MB-231, BGC-823 and MGC-803 cells.[16–18] However, its ability to reverse drug resistance has not been investigated.

In our present study, we investigated the reversal of FV-429 on hypoxic resistance to paclitaxel on human epithelial ovarian cancer cells and the mechanism of this resistance associated with c-Src axis regulation.

Results

Hypoxia deteriorated G2/M arrest induced by paclitaxel. Hypoxic culture condition was used to mimic the hypoxic environment in solid tumor. The resistance index (RI) was utilized as an item to access the resistance of cancer cells to drugs. It was considered resistant when RI was >2.0.[19] According to Figure 1a, IC_{50} was calculated according to cell growth inhibition. The IC_{50} of paclitaxel in hypoxic condition ($18.0 \pm 0.9\ \mu$M) was significantly higher than that in normoxic condition ($5.1 \pm 0.9\ \mu$M) on SK-OV-3 cells, and the same phenomenon was exerted on A2780 cells ($28.5 \pm 0.8\ \mu$M *versus* $8.3 \pm 0.9\ \mu$M). The RI was 3.5 on SK-OV-3 cell line and 3.4 on A2780 cell line. Cell cycle analysis was conducted to investigate if the resistance was related to cell cycle. As

[1]State Key Laboratory of Natural Medicines, Jiangsu Key Laboratory of Carcinogenesis and Intervention, China Pharmaceutical University, 24 Tongjiaxiang, Nanjing 210009, People's Republic of China; [2]Jiangsu Key Laboratory of Drug Design and Optimization, Department of Medicinal Chemistry, China Pharmaceutical University, 24 Tongjiaxiang, Nanjing 210009, People's Republic of China and [3]State Key Laboratory of Natural Medicines, Department of Natural Medicinal Chemistry, China Pharmaceutical University, 24 Tongjiaxiang, Nanjing 210009, People's Republic of China

*Corresponding author: L Zhao, School of Basic Medicine and Clinical Pharmacy, Jiangsu Key Laboratory of Carcinogenesis and Intervention, China Pharmaceutical University, 24 Tongjiaxiang, Nanjing 210009, People's Republic of China. Tel/Fax: +86 025 83271039; E-mail: zhaoli@cpu.edu.cn

[4]These authors contributed equally to this work.

Received 31.1.17; revised 15.6.17; accepted 04.7.17; Edited by M Daugaard

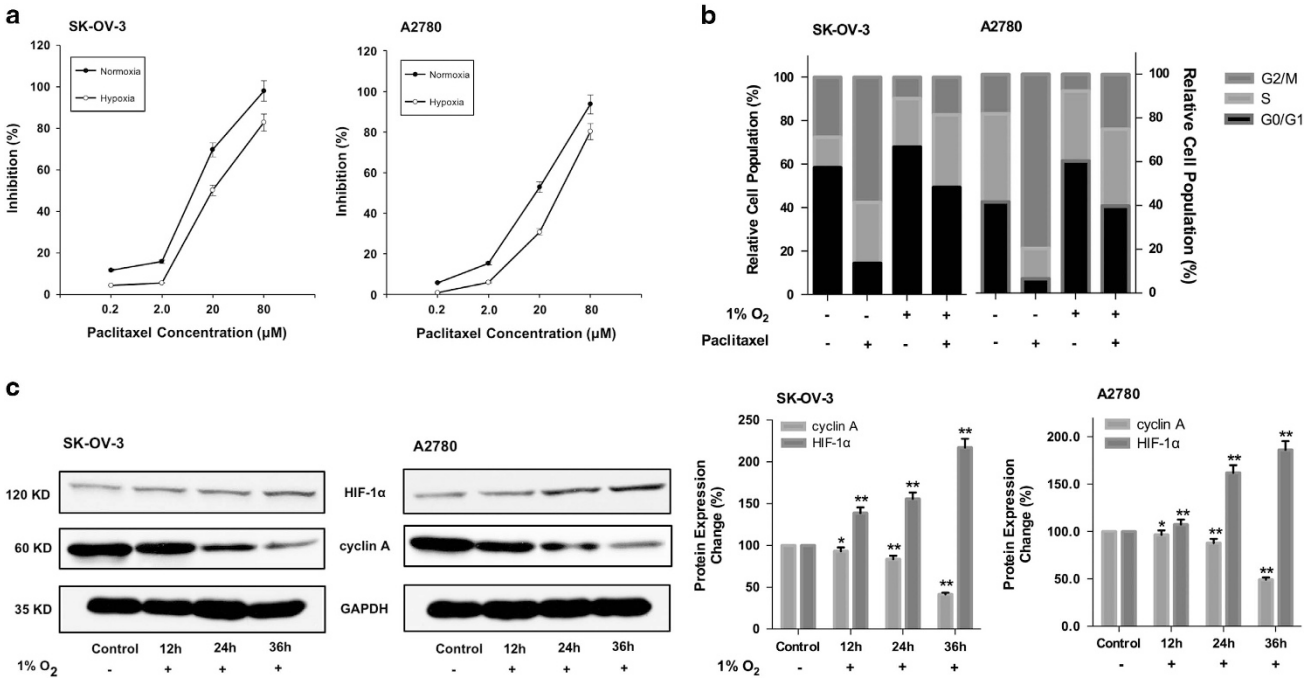

Figure 1 Hypoxia deteriorated G2/M arrest induced by paclitaxel. (**a**) Cell growth inhibition of paclitaxel treatment under normoxia and hypoxia assessed by MTT assay. Data had been statistically analyzed by Microsoft Excel 2013 and expressed as means ± S.D. for three independent experiments. (**b**) The influence of paclitaxel treatment on cell cycle under normoxia and hypoxia. Summary of the percentage of cells at G0/G1, S and G2/M phase was performed. (**c**) After 12, 24 and 36 h hypoxic incubation, cyclin A and HIF-1α expression detected by western blottings. Protein expression change was represented by densitometric analysis. The results are representative of three independent experiments and expressed as means ± S.D., $^{*}P<0.05$ and $^{**}P<0.01$, compared with the control groups

shown in Figure 1b, cell population at G2/M phase induced by paclitaxel of hypoxia groups was much smaller than that of the normoxia groups. Moreover in Figure 1c, during longer periods under hypoxia (12, 24, 36 h), cylin A, which was expressed at the end of G1 phase till the end of G2 phase and reached the highest during G2 phase,[20] was downregulated.

c-Src contributed to the resistance to paclitaxel under hypoxia. In order to investigate whether c-Src had an important role as a regulator, we added c-Src inhibitor dasatinib (dose selection indicated in Supplementary Figures S1 And S2) to the system and utilized c-Src small interfering RNA (siRNA) to silence CSK (gene of c-Src), as shown in Figures 2a and b, and the results illustrated that, with c-Src inhibition both at protein and gene levels, the sensitivity of cells to paclitaxel recovered from hypoxia. As hypoxic resistance to paclitaxel was associated with cell cycle, the influence of c-Src on cell cycle was examined. Figure 2c showed that paclitaxel-induced G2/M phase arrest under hypoxia was enhanced when CSK was knocked down. Moreover, in Figure 2d, with blockage of CSK in the paclitaxel-treated groups under hypoxia, the expression of cyclin B1 and the protein expression ratios of p-cdc25c/cdc25c and p-CDK1/CDK1 increased.

FV-429 enhanced the sensitivity to paclitaxel through G2/M arrest promotion. In order to investigate the reverse effect of FV-429 on hypoxic resistance to paclitaxel in ovarian cancer cells, proper doses should be chosen primarily. We first assessed the influence of FV-429 on cell viability of SK-OV-3 and A2780. As shown in Figure 3a, doses without severe proliferation inhibition were selected. To confirm that the doses we selected did not induce significant apoptosis, Annexin V/propidium iodide (PI) double staining assay was conducted. In Figure 3b, FV-429 at 5, 10 and 20 μM did not exhibit obvious apoptosis induction after 24 h treatment, with inhibition rates of 0.43, 0.24 and 0.27% on SK-OV-3 and 0.33, 0.14 and 0.35% on A2780. Figure 3c showed that 5, 10 and 20 μM FV-429 enhanced the sensitivity of the cells to paclitaxel under hypoxia in a dose-dependent manner. The data in Figure 3d showed that FV-429, combined with paclitaxel, significantly increased the percentage of the cells at G2/M phase under hypoxia in a dose-dependent manner. Furthermore, the expression of G2/M phase-related protein had been examined, as in Figure 3e, and the expression of cyclin B1 and the ratios of p-cdc25c/cdc25c and p-CDK1/CDK1 were upregulated.

FV-429 deteriorated c-Src/Stat3/HIF-1α pathway under hypoxia. From the results in Figure 4a, we found that, with higher doses of FV-429, the ratios of p-Src/c-Src and p-Stat3/Stat3 and HIF-1α expression were significantly downregulated compared with the hypoxic control groups. From the results, we realized that not only p-Src but also total c-Src was downregulated by FV-429. Thus we supposed that FV-429 might be able to suppress CSK. Comparing Figures 4b and c, FV-429 showed strong inhibition on CSK

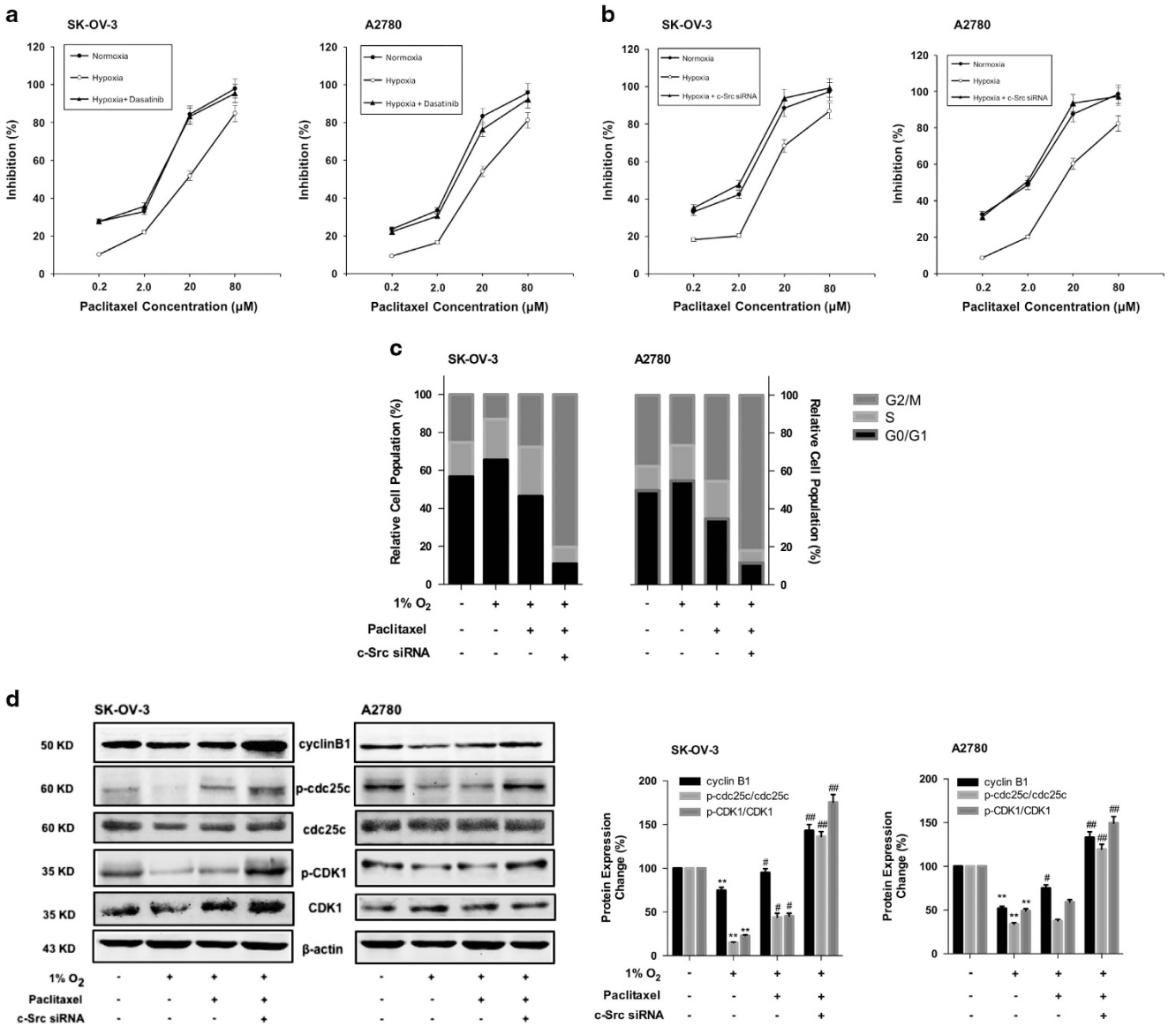

Figure 2 c-Src contributed to the resistance to paclitaxel under hypoxia. (**a**) The cell growth inhibition of paclitaxel combined dasatinib assessed by MTT assay. Data had been statistically analyzed by Microsoft Excel 2013 and expressed as means ± S.D. for three independent experiments. (**b**) Cell growth inhibition of paclitaxel on c-Src siRNA transfected cells assessed by MTT assay. Data had been statistically analyzed by Microsoft Excel 2013 and expressed as means ± S.D. for three independent experiments. (**c**) The influence of c-Src siRNA transfection on cell cycle with paclitaxel treatment under hypoxia. Summary of the percentage of cells at G0/G1, S and G2/M phase was performed. (**d**) The influence of c-Src siRNA transfection on the expression of cylin B1, p-cdc25c, cdc25c, p-CDK1 and CDK1 with paclitaxel treatment under hypoxia. Protein expression change was represented by densitometric analysis. The results are representative of three independent experiments and expressed as means ± S.D., $^{**}P<0.01$, compared with normoxia control groups and $^{\#}P<0.05$ and $^{\#\#}P<0.01$, compared with the hypoxia control groups

expression, which had significant difference from the dasatinib-treated groups ($P<0.01$), but less difference with c-Src siRNA-transfected groups ($P=0.046$).

Then we further investigated the influence of c-Src on Stat3/HIF-1α axis. In Figure 5a, the expression of Stat3 in the nucleus and the total expression of HIF-1α were significantly downregulated by FV-429. Furthermore, in Figure 5b, the signal of Stat3 in the nucleus was barely strong in the hypoxia control groups, while the effect was blocked by FV-429. Then we investigated the DNA-binding ability of Stat3. The results of electrophoretic mobility shift assay (EMSA) assay (Figure 5c) showed that FV-429 attenuated the binding ability of Stat3 to HIF-1α, which was enhanced in hypoxic condition.

FV-429 potentiated the effect and G2/M arrest induced by paclitaxel through c-Src/Stat3/HIF-1*α* pathway deterioration *in vivo*. Xenograft mouse model was utilized to assess the effect of combined treatment of mild dose of paclitaxel and FV-429. After treatment with FV-429 (10 mg/kg) and/or paclitaxel (5 mg/kg) for 14 days, the combined group showed stronger effect in tumor growth suppression (Figure 6a). According to the tumor weight analysis, the

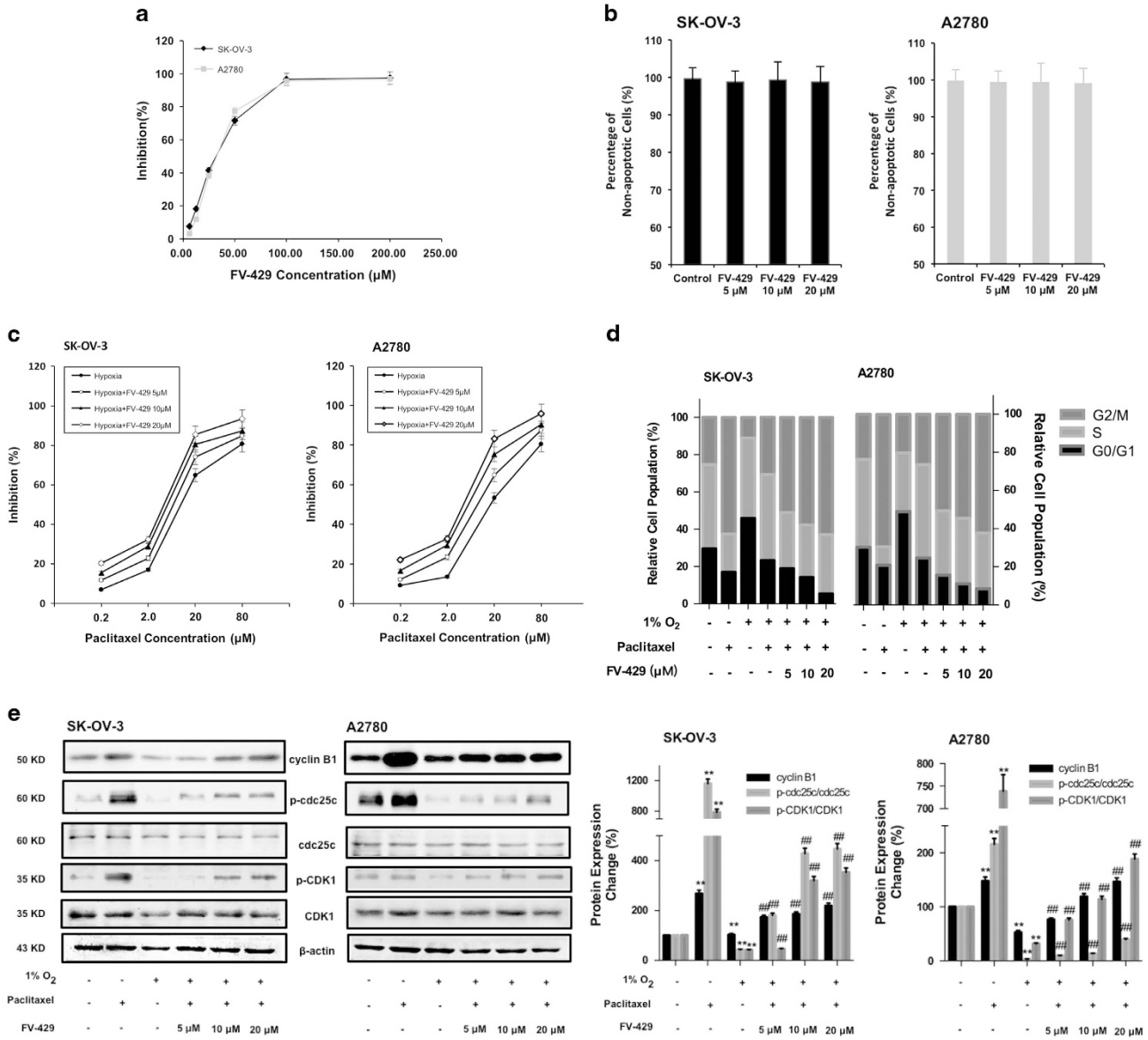

Figure 3 Mild doses of FV-429 enhanced paclitaxel-induced G2/M phase arrest under hypoxia. (**a**) The influence of FV-429 on cell growth inhibition assessed by MTT assay. Data had been statistically analyzed by Microsoft Excel 2013 and expressed as means ± S.D. for three independent experiments. (**b**) Percentage of non-apoptotic cells induced by 5, 10 and 20 μM FV-429 detected by Annexin V/PI double staining assay. Data had been statistically analyzed by Microsoft Excel 2013 and expressed as means ± S.D. for three independent experiments. (**c**) The influence of FV-429 on cell growth inhibition of paclitaxel under hypoxia assessed by MTT assay. Data had been statistically analyzed by Microsoft Excel 2013 and expressed as means ± S.D. for three independent experiments. (**d**) The influence of FV-429 on cell cycle with paclitaxel treatment under hypoxia. Summary of the percentage of cells at G0/G1, S and G2/M phase was performed. (**e**) The influence of FV-429 on the expression of cylin B1, p-cdc25c, cdc25c, p-CDK1 and CDK1 with paclitaxel treatment under hypoxia. Protein expression change was represented by densitometric analysis. The results are representative of three independent experiments and expressed as means ± S.D., $^{**}P<0.01$, compared with normoxia control groups and $^{\#\#}P<0.01$, compared with the hypoxia control groups

inhibition rate of 10 mg/kg FV-429 combined with 5 mg/kg paclitaxel group was 57.50%, which was much better than FV-429 single treated group (32.14%) and paclitaxel group (31.06%).

We also confirm the effect of FV-429 on paclitaxel-induced G2/M phase arrest *in vivo*. As shown in Figure 6b, the expression of cylin B1 and the ratios of p-cdc25c/cdc25c and p-CDK1/CDK2 were significantly upregulated in the combined treated group. Moreover, the results of immunohistochemistry (IHC; Figure 6c) suggested that, in the combination group, there were significant increase of cyclin A and cyclin B1 and strong suppression on ki67 nuclear translocation.

Then we confirm the potentiated effect of FV-429 on c-Src/Stat3/HIF-1α pathway *in vivo*. As shown in Figure 6d, after FV-429 treatment, the protein expression ratios of p-Src/c-Src and p-Stat3/Stat3 and HIF-1α expression decreased in hypoxic tumor tissues (the central part of tumors and normoxic tumor tissues referred to the outer part of tumors[21]), and IHC study (Figure 6e) showed the expression of c-Src and HIF-1α and nuclear translocation of Stat3 decreased in the tissues.

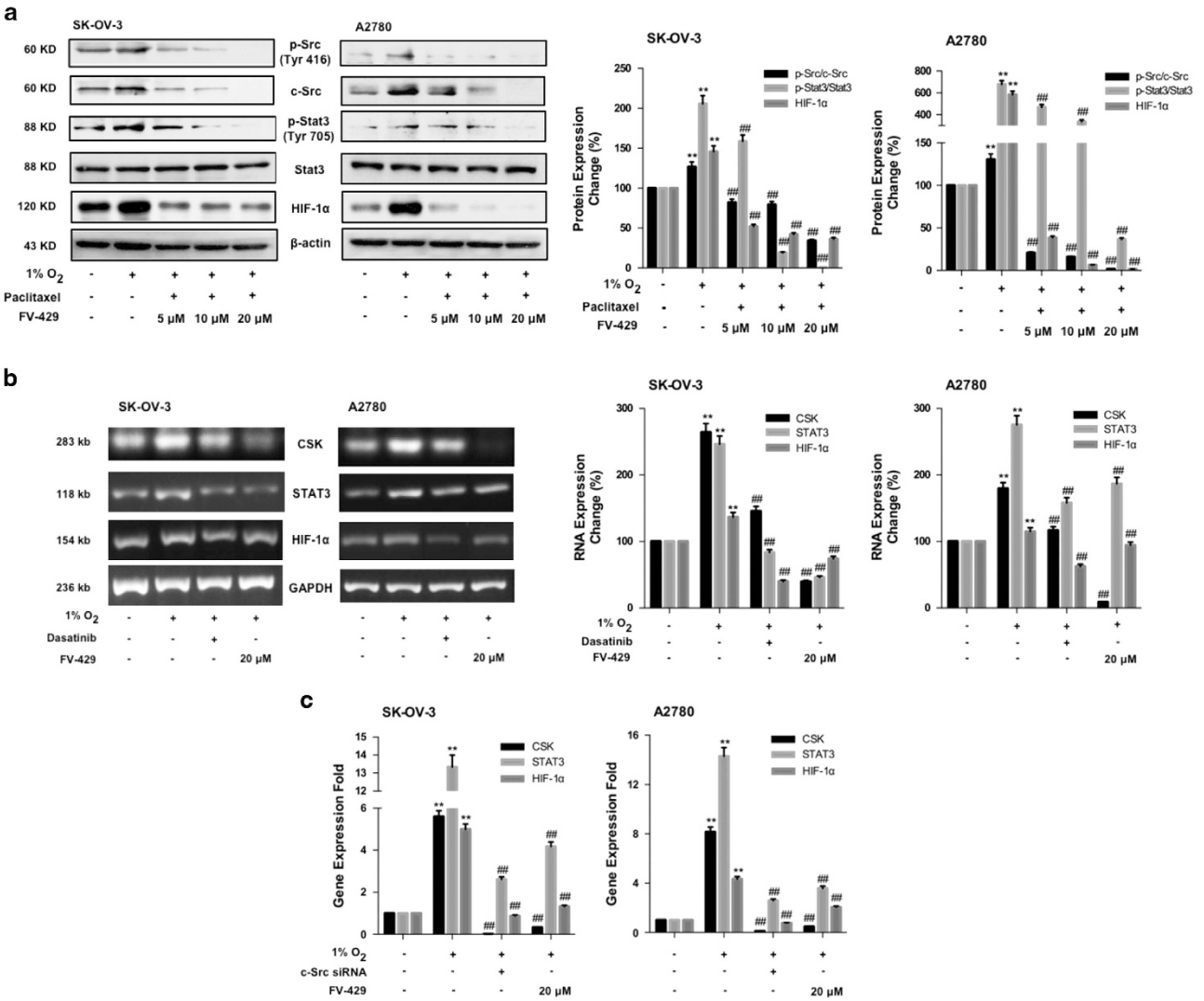

Figure 4 FV-429 suppressed c-Src/Stat3/HIF-1α pathway and c-Src mRNA expression. (**a**) The influence of FV-429 on p-Src (Tyr 416), c-Src, p-Stat3 (Tyr 705), Stat3 and HIF-1α expression with paclitaxel treatment under hypoxia. Protein expression change was represented by densitometric analysis. The results are representative of three independent experiments and expressed as means $\pm$ S.D., $^{**}P<0.01$, compared with normoxia control groups and $^{\#\#}P<0.01$, compared with the hypoxia control groups. (**b**) The influence of FV-429 on mRNA expression of CSK, STAT3 and HIF-1α detected by electrophoresis on 3% agarose gel. RNA expression change was represented by densitometric analysis. The results are representative of three independent experiments and expressed as means $\pm$ S.D., $^{**}P<0.01$, compared with normoxia control groups and $^{\#\#}P<0.01$, compared with the hypoxia control groups. (**c**) The influence of FV-429 on mRNA expression of CSK, STAT3 and HIF-1α detected by reverse transcriptase PCR. Data had been statistically analyzed and displayed in column charts as means $\pm$ S.D. for three independent experiments by Graphpad Prism 6.0c, $^{**}P<0.01$, compared with the normoxia control groups and $^{\#\#}P<0.01$, compared with the hypoxia control groups

Toxicological assessment. We investigated the influence of FV-429 single or paclitaxel combined treatment on animals' weight, main organs and peripheral blood. As shown in Figure 7a, there was a significant decrease of animals' weight of mice in the paclitaxel single group, but in FV-429 single or combined group, the effect was mild. And the results of hematoxylin and eosin staining of the five main organs of an individual showed that both paclitaxel and FV-429 exerted no significant toxicities (Figure 7b). Moreover, paclitaxel treatment resulted in an increase of band neutrophils and decrease of monocytes and total white blood cells, but in FV-429 single or combined groups, the trend was improved (Table 1).

Discussion

In the present study, we demonstrated that hypoxic condition rendered resistance to paclitaxel in human epithelial ovarian cancer cells through deteriorating paclitaxel-induced G2/M phase arrest. Blockage of c-Src can significantly improve the sensitivity of the cells to paclitaxel under hypoxia and paclitaxel-induced G2/M arrest. Further study revealed that flavonoid compound FV-429 suppressed gene expression and protein activation of c-Src under hypoxic condition. With c-Src suppression by FV-429, the translocation of Stat3 into nucleus and its binding to HIF-1α was inhibited, leading to paclitaxel-induced G2/M phase enhancement. Also we demonstrated that FV-429, combined with paclitaxel, exerted better

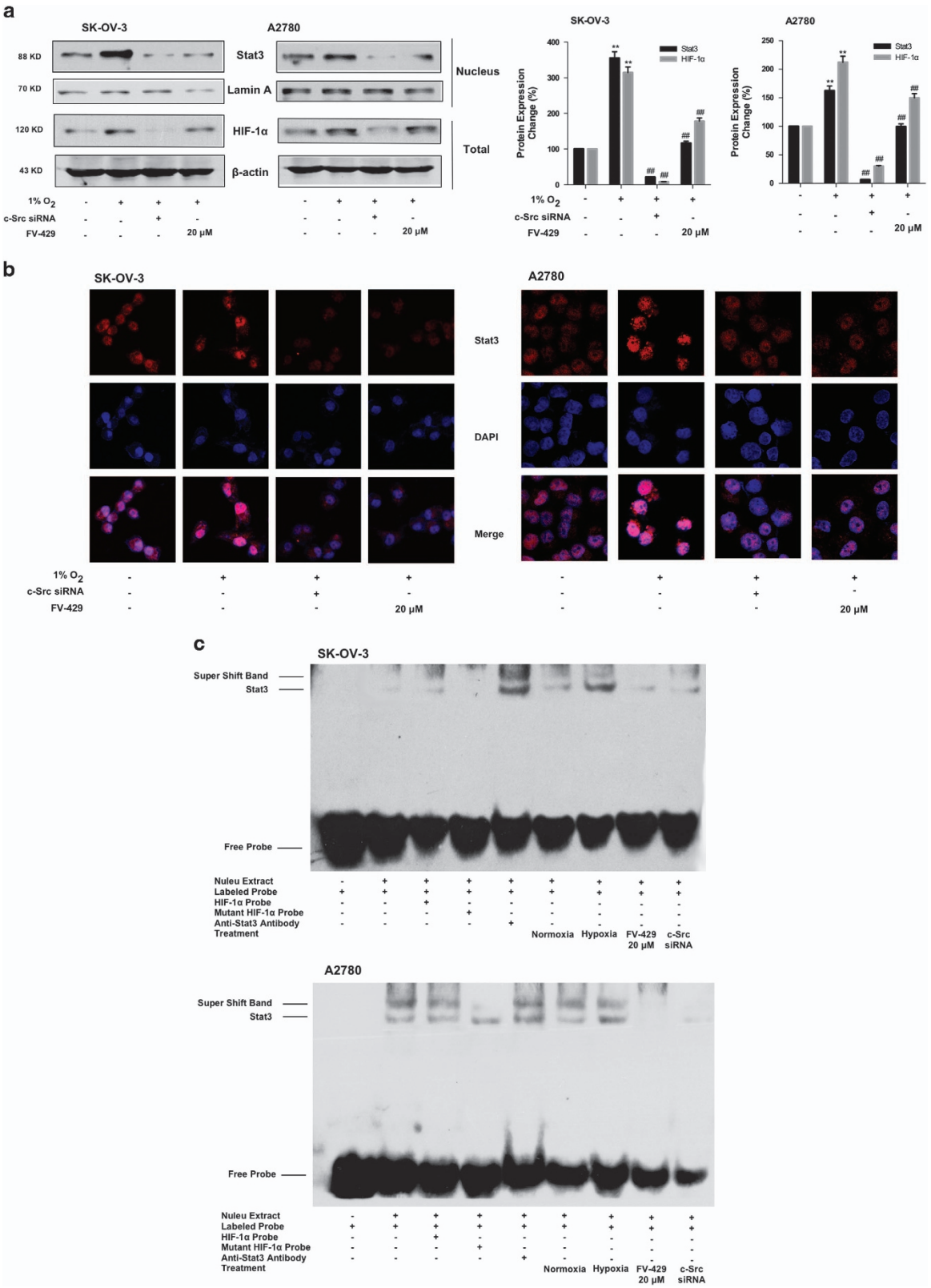

Figure 5 FV-429 inhibited Stat3 nuclear translocation and binding to HIF-1α. (**a**) The influence of FV-429 on nuclear expression of Stat3 and total expression of HIF-1α under hypoxia. Protein expression change was represented by densitometric analysis. The results are representative of three independent experiments and expressed as means $\pm$ S.D., $^{**}P<0.01$, compared with the normoxia control groups and $^{\#\#}P<0.01$, compared with the hypoxia control groups. (**b**) The influence of FV-429 on Stat3 nuclear translocation examined by immunofluorescence (×600). (**c**) The influence of FV-429 on binding ability of Stat3 to HIF-1α under hypoxia assessed by EMSA

antixenograft tumor effect than both single treated groups *in vivo*, with hematological side effects' improvement and no toxicity on animals' main organs.

Among gynecological malignancies, ovarian cancer is the most difficult to cure.[22] Maximum debulking surgery followed by chemotherapy consisting of paclitaxel and platinum is the standard treatment for advanced ovarian cancer.[23] Though $>70\%$ of the patients responded to chemotherapy initially, the majority relapsed.[22] Recently, there is growing evidence highlighting the importance of tumor microenvironment-mediated chemoresistance mechanisms in ovarian cancer.[24] It has long been noted that the rapidly proliferating malignant cells generates greater oxygen consumption, which jointly favor the formation of hypoxic areas within the solid tumors.[25] Cycling hypoxia is a well-recognized phenomenon within solid tumors that contributes to the resistance to chemotherapy or radiotherapy.[26] Studies demonstrated that cells in hypoxic regions tend to be arrested at G1 phase.[9,27,28] Paclitaxel was found to stabilize cytoplasmic microtubules, thus the cells would stagnate at the beginning of M phase, followed by induction of apoptosis and/or mitotic catastrophe.[29] According to our results, the antiproliferative effect of paclitaxel was attenuated under hypoxia (Figure 1a), with IC_{50} increasing around threefolds. And cell cycle analysis showed a decrease of G2/M phase population in the paclitaxel-treated group under hypoxia (Figure 1b). Considering these, we may safely conclude that hypoxic region in ovarian cancer contributed to the resistance by inhibiting paclitaxel-induced G2/M phase arrest.

Abnormal expression or activation of CSK has been documented to have vital roles in tumor malignancy and interacted with mechanisms that regulate paclitaxel sensitivity.[29] Thus we wondered whether c-Src/Stat3/HIF-1α pathway was also aroused in hypoxic resistance to paclitaxel. As we discovered, with both c-Src activation suppression (Figure 2a) and CSK blockage (Figure 2b), the antiproliferative ability of paclitaxel under hypoxia has been greatly improved. Moreover, the cell population at G2/M phase, as well as G2/M phase-specific protein expression, significantly increased (Figure 2c) with CSK silenced (Figure 2d). All these indicated that blockage of c-Src improve ovarian cancer cells' sensitivity to paclitaxel under hypoxia, thus c-Src may serve as a promising target to overcome hypoxic resistance to paclitaxel in ovarian cancer.

Studies showed that active c-Src promoted HIF-1α function by activating Stat3, which bind to and activated HIF-1α promoter, resulting in downstream effects.[30,31] From the results of Figures 4a and c, Src/Stat3/HIF-1α pathway was activated under hypoxia, and the activation was suppressed by FV-429 treatment. From the results, we noticed that not only activated p-Src (phosphorylated at Tyr 416) but also total c-Src decreased. Therefore, we supposed that FV-429 might be able to suppress c-Src gene expression. Comparing the results of Figures 4b and c, the suppression of CSK by FV-429 exhibited less variation with that of c-Src siRNA transfection groups. Besides, with c-Src gene suppression by FV-429, the nuclear translocation of Stat3 has also been blocked (Figures 5a and b), as well as the binding of Stat3 to HIF-1α (Figure 5c). And the expression of Hexokinase II and VEGF, both downstream targets of HIF-1α, decreased, further indicating the suppression on HIF-1α function (Supplementary Figure S3). Moreover, *in vivo* results indicated that FV-429 inactivated c-Src/Stat3/HIF-1α pathway in hypoxic tumor tissues (Figures 6d and e) and FV-429, combined with paclitaxel, induced significant increased G2/M-specific protein expression in tumor tissues (Figures 6b and c) with an inhibition rate of 57.5%, confirming the effectiveness of FV-429 in improving paclitaxel treatment by G2/M phase arrest enhancement through c-Src/Stat3/HIF-1α pathway *in vivo*.

It has been proposed that chemotherapeutic drugs effectively trigger mitotic catastrophe at low doses, significantly limiting side effects.[32] The side effect of paclitaxel include allergic reaction, neurotoxicity and so on[33] but the more common one was hematological toxicity.[34] As we demonstrated in Table 1, there was a decrease of monocytes and increase of band neutrophils in the paclitaxel single treated group, indicating myelosuppression and immunosuppression existence. However, in groups with FV-429 treatment, the influence was weakened. As it was reported that flavonoids were able to serve as xenobiotics that are metabolized by the cytochrome P-450 enzymes and conjugating protective enzymes,[35] we speculated that the effect might be attributed to the protective effect of flavonoids. Besides, flavonoids metabolized slowly *in vivo*,[36] suggesting a longer treating period.

The mechanism we investigated here focused on the influence of c-Src/Stat3/HIF-1α pathway regulation on cell cycle. However, whether the mechanism also affects other pharmacological effects induced by paclitaxel, for instance, autophagy, still remained a problem to resolve.

In summary, the present study discovered that c-Src contributed to hypoxic microenvironment-rendered paclitaxel resistance in human epithelial ovarian cancer cells by G2/M phase arrest deterioration, and through c-Src suppression, FV-429 was capable of reversing the resistance by blocking the c-Src/Stat3/HIF-1α pathway. Our study provided a new thinking of c-Src suppression in cancer therapy and a promising agent in this field.

Materials and Methods

Reagents. FV-429 (MW 429) was prepared by Dr. Zhiyu Li, dissolved in dimethyl sulfoxide (DMSO, Sigma-Aldrich, St. Louis, MO, USA) to 100 mM and stored at -20 °C.

Paclitaxel injection was purchased from Taiji Pharmaceutical Co. Ltd. (Sichuan, China) as stocking solution and diluted with RPMI-1640 (Gibco, Carlsbad, CA, USA) and DMEM (Gibco) medium to a final concentration with organic solute no more than 0.1%. Dasatinib (Sigma-Aldrich) was diluted with DMSO to 100 μM and stored at -20 °C. The drug was freshly diluted with RPMI-1640 and DMEM medium to 0.05 μM before use. MTT (3-(4,5-dimethylthiazol-2-yl)-2,5- diphenytetrazoliumbromide) was obtained from Fluka Chemical Corp. (Ronkonkoma, NY, USA) and was dissolved in 0.01 M phosphate-buffered saline (PBS).

Antibodies against c-Src, HIF-1α, Stat3, p-Stat3 (Tyr705), Cyclin B1and GAPDH were products of Bioworld Technology (St. Louis Park, MN, USA). Antibodies against p-Src (Tyr416), p-cdc25c (Ser216) and cdc-25c were products of Cell Signaling Technology (Beverly, MA, USA). Antibodies against Cyclin A, cdc-2 and p-cdc2 (Thr161) were products of Santa Cruz Biotechnology (Santa Cruz, CA, USA). Normal mouse and rabbit IgG-HRB secondary antibody were purchased from Santa Cruz Biotechnology.

Cell culture. SK-OV-3 (human epithelial ovarian cancer) cells were originally from the Cell Bank of the Shanghai Institute of Biochemistry and Cell Biology, Chinese Academy of Sciences (Shanghai, China). A2780 (human epithelial ovarian

cancer) cells were originally from KeyGen Biotechnology (Nanjing, China). SK-OV-3 cells were grown in RPMI-1640, and A2780 were in DMEM; all media contained 10% heat-inactivated fetal bovine serum (Wisent, St. Bruno, Quebec, Canada). All cells were incubated in a humidified atmosphere at 37 °C.

siRNA transient transfection. C-Src siRNA was purchased from Santa Cruz Biotechnology. SiRNA transfections were performed according to the manufacturer's instructions using Lipofectamine 2000 reagent (Invitrogen, Carlsbad, CA, USA). After that, the transfected system was removed, and it

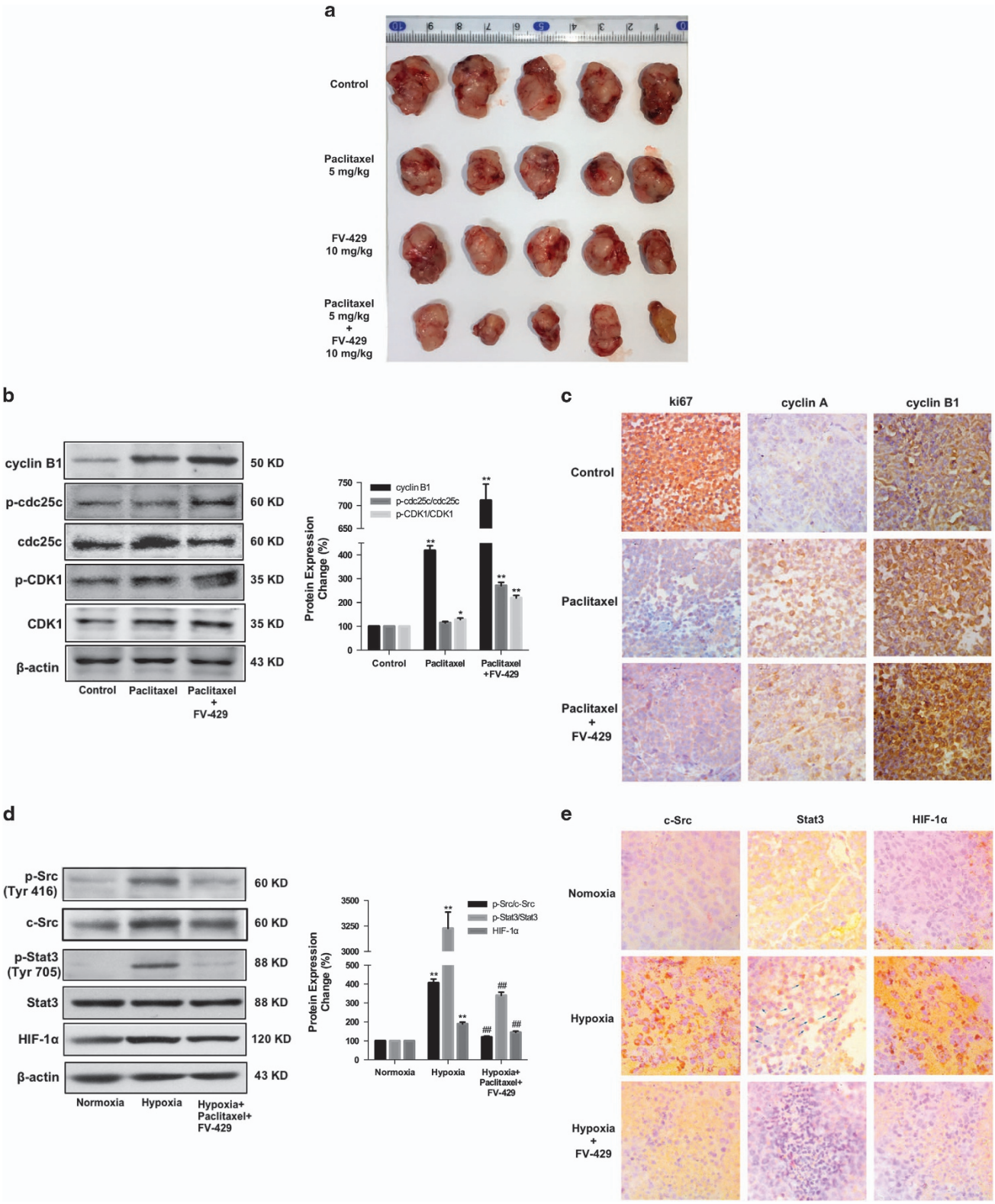

was not until 24 h cultured in normal media were the cells used for further experiment.

Normoxic and hypoxic culture conditions. Cells were maintained at 37 °C in humidified incubator containing 20% O_2, 5% CO_2 and 75% N_2 in normoxia. Hypoxic condition were achieved at 37 °C by culturing cells in a modified incubator chamber flushed with a gas mixture containing 1% O_2, 94% N_2 and 5% CO_2 in a humidified atmosphere.

MTT assay. Cell viability was measured using the MTT assay. Cells (8×10^3) were treated with FV-429 and/or paclitaxel for 24 h at various concentrations. Absorbance (A) of the final formazan was measured spectrophotometrically at 570 nm by Universal Microplate Reader EL800 (BioTek Instruments, Winooski, VT, USA). The inhibition ratio (%) was calculated as $((A_{control} - A_{treated})/A_{control}) \times 100\%$. $A_{treated}$ and $A_{control}$ are the average absorbance values of three parallel experiments from treated and control groups, respectively. RI was calculated as the IC_{50} of SK-OV-3 and A2780 cells under hypoxia/normoxia.

Annexin V/PI staining. SK-OV-3 and A2780 cells were harvested and stained with the Annexin V/PI Cell Apoptosis Detection Kit (KeyGen Biotechnology) according to the manufacturer's instructions. Data were acquired from flow cytometry CellQuest Software (Becton Dickinson (Franklin Lakes, NJ, USA)) and analyzed by FlowJo version 10 (Ashland, OR, USA).

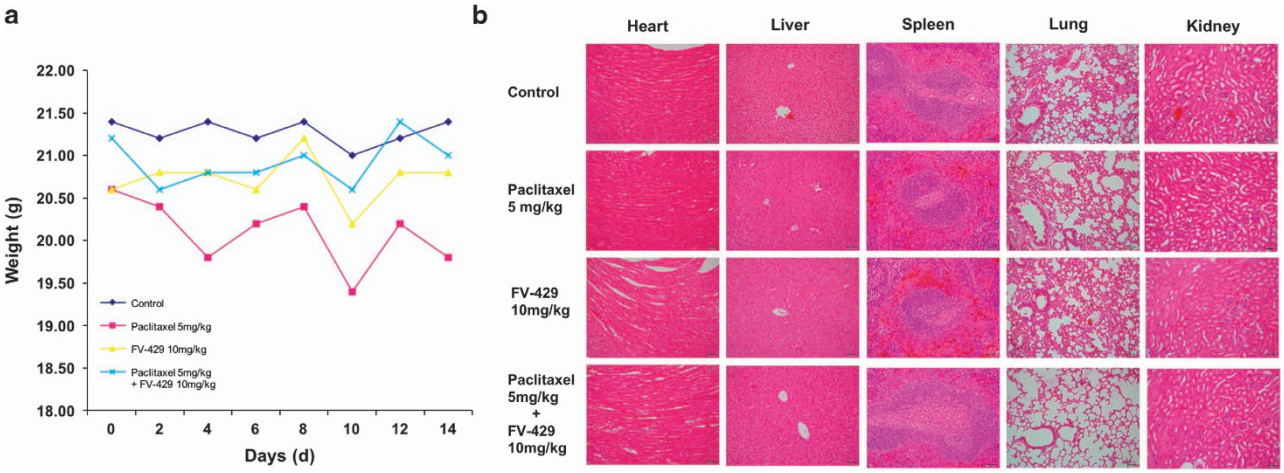

Figure 7 Toxicological assessment. (**a**) Body weight change of xenografted nude mice by days. Data had been statistically analyzed by Microsoft Excel 2013 and expressed as means ± S.D. ($n = 5$). (**b**) The influence of FV-429 and paclitaxel single or combined treatment on the heart, liver, spleen, lung and kidney was examined by hematoxylin and eosin staining (×200)

Table 1 Hematology profile

Hematological parameter	Control	Paclitaxel (5 mg/kg)	FV-429 (10 mg/kg)	Paclitaxel +FV-429	Standard
White blood cells (×10^3 μl)	11.09/12.99	4.06/4.08	6.09/7.52	7.34/8.18	4.5–9.1
Red blood cells (×10^3 μl)	10.80/10.55	9.47/9.76	10.15/10.06	11.64/10.17	7.51–16.1
Hemoglobin (g/l)	154/154	145/148	156/139	158/157	126–161
Platelets (×10^3 μl)	467/488	472/442	425/502	523/535	115–1037
Band neutrophils (%)	3.54/4.50	18.80/20.40	3.84/5.14	6.50/9.40	0–1
Lymphocytes (%)	91.74/90.60	79.20/78.20	94.94/91.84	87.60/87.40	49–82
Monocytes (%)	4.64/4.74	1.84/1.24	4.34/3.94	5.64/4.04	2–8
Eosinophils (%)	0.14/0.14	0.04/0.24	0.04/0.14	0.14/0.04	0–3
Basophils (%)	0.14/0.14	0.24/0	0.04/0.14	0.14/0.14	0–3
Mean corpuscular volume (fl)	43.3/45.6	46.8/45.7	46.0/44.5	44.8/45.2	41–60
Hematocrit (%)	46.8/48.1	44.3/44.6	46.7/44.8	52.2/46.0	34–50
Mean corpuscular hemoglobin (pg)	14.3/14.6	15.3/15.2	15.4/13.8	15.3/15.4	13–19
Mean corpuscular hemoglobin concentration (%)	329/320	327/332	334/310	341/341	316–354

Two mice of each group were used. Standard ranges were obtained in-house from 100 normal BALB/c nude mice aged 8–12 weeks

Figure 6 Antixenografted tumor effect and reversal mechanism of FV-429 combined with paclitaxel *in vivo*. (**a**) Image of the resected xenografted tumors. (**b**) Expression of cylin B1, p-cdc25c, cdc25c, p-CDK1 and CDK1 in hypoxic regions of xenografted tumors detected by western blottings. Protein expression change was represented by densitometric analysis. The results are representative of three independent experiments and expressed as means ± S.D., $^*P < 0.05$ and $^{**}P < 0.01$, compared with the control groups. (**c**) Expression of ki67, cylin A and cylin B1 in hypoxic regions of xenografted tumors detected by immunohistochemistry (×400). (**d**) Expression of p-Src (Tyr 416), c-Src, p-Stat3 (Tyr 705), Stat3 and HIF-1α in normoxic and hypoxic regions of xenografted tumors detected by western blottings. Protein expression change was represented by densitometric analysis. The results are representative of three independent experiments and expressed as means ± S.D., $^{**}P < 0.01$, compared with the normoxia control groups and $^{\#\#}P < 0.01$, compared with the hypoxia control groups. (**e**) Expression of c-Src, Stat3 and HIF-1α in normoxic and hypoxic regions detected by immunohistochemistry (×400). Arrows referred to Stat3 nuclear translocation

Table 2 Primer sequences used in the study

Gene symbol	Organism	Forward primer (5′ → 3′)	Reverse primer (5′ → 3′)
CSK	*Homo sapiens*	TCCGGCCCCGTCTCTCTTGG	ACCCTCACGGGCAGGACAGG
STAT3	*Homo sapiens*	ACCAACAATCCCAAGAATGT	CGATGCTCAGTCCTCGC
HIF-1α	*Homo sapiens*	CCTTTGGCTCTTCAGGATGC	GGTCTTTCTGCACATTTGGGTGG
GAPDH	*Homo sapiens*	GGTGTGAACCATGAGTATGACAAC	CCAGTGAGGCAGGGATGATGTTC

Cell cycle analysis. SK-OV-3 and A2780 cells were weeded into a six-well plate at 2.5×10^5 cells per well. The cells were incubated for 24 h in serum-free medium and treated with or without FV-429 and/or paclitaxel for another 24 h in normoxia or hypoxia. Then the cells were harvested and fixed in cold 70% ethanol overnight at 4 °C. After washing with PBS, cells were incubated with 100 μl RNaseA (KeyGen Biotechnology) at 37 °C for 30 min. Subsequently, cells were incubated with 400 μl PI (KeyGen Biotechnology) for 30 min at 4 °C in the dark and detected by flow cytometry (Becton Dickinson). Data were analyzed by FlowJo version 10.

Extraction of cytoplasmic and nuclear fractions. SK-OV-3 and A2780 cells were treated with FV-429 and/or paclitaxel at the indicated concentrations for 24 h. Nuclear and cytosolic protein extract were prepared using a Nuclear/Cytosol Fractionation Kit (BioVision, Mountain View, CA, USA) according to the manufacturer's protocol. One part of the cytosolic and nuclear extract was used for EMSA. Final detection was performed with western blotting analysis.

Western blotting analysis. Cells were collected after the operation previously mentioned and then lysed in lysis buffer. Nuclear and cytoplasmic proteins of the cells were extracted as previously mentioned. Protein samples were loaded onto an SDS-PAGE gel and transferred to a nitrocellulose membrane (BioTrace NT; PallCor, Arroyto, Cordoba, Argentina). The membranes were then blocked with 3% fat-free milk in PBST for 1 h and incubated with primary antibodies overnight at 4 °C followed by IgG-HRB secondary antibody for 1 h at room temperature. Detection was performed by X-ray films. All blots were stripped and reprobed with polyclonal anti-GAPDH, anti-β-actin or anti-lamin A antibody to ascertain loading of proteins.

Immunofluorescence confocal microscopy. Treated SK-OV-3 and A2780 cells were harvested and seeded onto glass coverslips processed for immunofluorescence. The glass coverslips were washed twice with cold PBS for 5 min, fixed with 4% paraformaldehyde for 30 min and incubated with 0.3% Triton X-100 for 10 min. After incubation, the cell were blocked with PBS containing with 1% bovine serum albumin for 1 h and incubated with anti-Stat3 antibody at 4 °C overnight. After being washed with PBS for three times, the cells were stained with FITC-conjugated anti-rabbit IgG antibody for 1 h at room temperature. And then the coverslips were stained with diamidinophenylindole for 10 min. The images were captured with an Olympus FV1000 confocal microscope (Tokyo, Japan).

Electrophoretic mobility shift assay. Nuclear extracts were prepared as described above. According to the manufacturer's instructions, nonradioactive (biotin label) gel shift assays were performed. In brief, oligonucleotide proves were synthesized, annealed and labeled using the Biotin 3′-END DNA Labeling Kit (Pierce, Waltham, MA, USA). The binding reactions were performed according to the manufacturer's protocol. Finally, the chemiluminescence of the biotin-labeled DNA was detected using the Chemiluminescent EMSA Kit (Beyotime, Nanjing, Jiangsu, China) and the samples were exposed to X-ray film.

Analysis of mRNA levels. Cells were harvested after 24 h treatment with dasatinib or FV-429 under hypoxia. Cells that were not treated with the agents were utilized as control group of normoxia or hypoxia. Total RNA was extracted from each sample with Trizol (Takara Biotech, Dalian, China) according to the manufacturer's instructions. cDNA was synthesized from the isolated RNA by RT and amplified individually by PCR (primer sequences are listed in Table 2).

Xenografted mouse model. Five-to-6-week-old female BALB/c nude mice were purchased from SLAC laboratory Animals (Shanghai, China) and were raised in air-conditioned rooms with 12 h light per day and fed with standard laboratory food and water. The transplanted tumors were induced by subcutaneous injection into the flanks of the mice with 1.0×10^6 A2780 cells. After 12–14 days, the tumor volume was measured by micrometer calipers, and the mice with similar tumor sizes were randomly divided into four groups with five individuals per group. The mice were treated with 5 mg/kg paclitaxel or/and 10 mg/k paclitaxel every 2 days. After 2 weeks, the mice were killed, and the tumor xenografts were removed and measured. Tumor volume (TV) was calculated using the following formula: TV (mm^3) = $D/2 \times d^2$, where D is the longest diameter while d is the shortest diameters. This study was approved in SPF Animal Laboratory of China Pharmaceutical University. The animals were weighed every 2 days and monitored for mortality throughout the experimental period to assess toxicity of the treatment.

Immunohistochemistry. The expression of ki67 (KeyGen Biotechnology), cylin A and cylin B1, as well as c-Src, Stat3 and HIF-1α, in tumor tissues of nude mice were assessed as described previously[37] by goat-anti-mouse antibodies and an Ultra-Sensitive TMSAP Kit (Kit 9710 Maixin, Fuzhou, Fujian, China). All reagents were supplied by Maixin-Bio Co, Fuzhou, China.

Statistical analysis. Data shown were presented by means $\pm$ S.D. from triplicate experiments performed in a parallel manner unless otherwise indicated. Statistical analysis was performed using an unpaired two-tailed Student's *t*-test.

Conflict of Interest

The authors declare no conflict of interest.

Acknowledgements. This work was supported by the National Natural Science Foundation of China (Nos. 81473231, 81373449) and Science Foundation for Distinguished Young Scholars of Jiangsu Province (BK20150028), Jiangsu Qing Lan Project, the National Science & Technology Major Project (No. 2012ZX09304-001, No. 2013ZX09103-001-007), Program for Changjiang Scholars and Innovative Research Team in University (IRT1193), the Project Program of State Key Laboratory of Natural Medicines, China Pharmaceutical University (SKLNMZZCX201606).

Publisher's Note

1. Lee H, Lee T, Lee N, Yang GE, Lee C, Lee J *et al.* Src activates HIF-1α not through direct phosphorylation of HIF-1a-specific prolyl-4 hydroxylase 2 but through activation of the NADPH oxidase/Rac pathway. *Carcinogenesis* 2011; **32**: 703–712.
2. Ng KP, Manjeri A, Lee KL, Huang W, Tan SY, Chuah CTH *et al.* Physiologic hypoxia promotes maintenance of CML stem cells despite effective BCR-ABL1 inhibition. *Blood* 2015; **123**: 3316–3326.
3. Semenza GL. Hypoxia-inducible factors in physiology and medicine. *Cell* 2012; **148**: 399–408.
4. Simon MC, Keith B. The role of oxygen availability in embryonic development and stem cell function. *Nat Rev* 2008; **9**: 285–296.
5. Zhao L, Li W, Zhou YX, Zhang Y, Huang SL, Xu XF *et al.* The overexpression and nuclear translocation of Trx-1 during hypoxia confers on HepG2 cells resistance to DDP, and GL-V9 reverses the resistance by suppressing the Trx-1/Ref-1 axis. *Free Radic Biol Med* 2015; **82**: 29–41.
6. Li H, Zeng J, Shen K. PI3K/AKT/mTOR signaling pathway as a therapeutic target for ovarian cancer. *Arch Gynecol Obstet* 2014; **2014**: 1067–1078.
7. Birner P, Schindl M, Obermair A, Breitenecker G, Oberhuber G. Expression of hypoxia-inducible factor 1a in epithelial ovarian tumors: its impact on prognosis and on response to chemotherapy. *Clin Cancer Res* 2001; **7**: 1661–1668.
8. Nakai H, Watanabe Y, Ueda H, Hoshiai H. Hypoxia inducible factor 1-α expression as a factor predictive of efficacy of taxane/platinum chemotherapy in advanced primary epithelial ovarian cancer. *Cancer Lett* 2007; **251**: 164–167.

9. Huang L, Ao Q, Zhang Q, Yang X, Xing H, Li F *et al.* Hypoxia induced paclitaxel resistance in human ovarian cancers via hypoxia-inducible factor 1a. *J Cancer Res Clin Oncol* 2010; **2010**: 447–456.
10. Gray MJ, Zhang J, Ellis LM, Semenza GL, Evans DB, Watowich SS *et al.* HIF-1a, STAT3, CBP/p300 and Ref-1/APE are components of a transcriptional complex that regulates Src-dependent hypoxia-induced expression of VEGF in pancreatic and prostate carcinomas. *Oncogene* 2005; **2005**: 3110–3120.
11. Mukhopadhyay D, Tsiokas L, Zhou X, Foster D, Brugge JS, Sukhatme PV. Hypoxia induction of human vascular endothelial growth factor expression through c-Src activation. *Nature* 1995; **375**: 577–581.
12. Suwaki N, Vanhecke E, Atkins KM, Graf M, Swabey K, Huang P *et al.* A HIF-regulated VHL-PTP1B-Src signaling axis identifies a therapeutic target in renal cell carcinoma. *Sci Transl Med* 2011; **3**: 85ra47.
13. Sievers E, Trautmann M, Kindler D, Huss S, Gruenewald I, Dirksen U *et al.* SRC inhibition represents a potential therapeutic strategy in liposarcoma. *Int J Cancer* 2015; **137**: 2578–2588.
14. McCann GA, Naidu S, Rath KS, Bid HK, Tierney BJ, Suarez A *et al.* Targeting constitutively-activated STAT3 in hypoxic ovarian cancer, using a novel STAT3 inhibitor. *Oncoscience* 2014; **1**: 216–228.
15. Wu X, Zhang H, Salmani JMM, Fu R, Chen B. Advances of wogonin, an extract from *Scutellaria baicalensis*, for the treatment of multiple tumors. *Oncotargets Ther* 2016; **2016**: 2935–2943.
16. Yang Z, Qiang L, Wu T, Chen F, Yang H, Zhao Q *et al.* Reactive oxygen species–mitochondria pathway involved in FV-429-induced apoptosis in human hepatocellular carcinoma HepG2 cells. *Anticancer Drugs* 2011; **22**: 886–895.
17. Zhou Y, Wei L, Zhang H, Dai Q, Li Z, Yu B *et al.* FV-429 induced apoptosis through ROS-mediated ERK2 nuclear translocation and p53 activation in gastric cancer cells. *J Cell Biochem* 2015; **116**: 1624–1637.
18. Zhou Y, Lu N, Qiao C, Ni T, Li Z, Yu B *et al.* FV-429 induces apoptosis and inhibits glycolysis by inhibiting Akt-mediated phosphorylation of hexokinase II in MDA-MB-231 cells. *Mol Carcinog* 2015; **9999**: 1–12.
19. Shi LX, Ma R, Lu R, Xu Q, Zhu Z, Wang L *et al.* Reversal effect of tyroservatide (YSV) tripeptide on multi-drug resistance in resistant human hepatocellular carcinoma cell line BEL-7402/5-FU. *Cancer Lett* 2008; **269**: 101–110.
20. Santoa L, Siua KT, Rajea N. Targeting cyclin-dependent kinases and cell cycle progression in human cancers. *Semin Oncol* 2015; **42**: 788–800.
21. Li Y, Fu L, Li J, Qin Y, Zeng T, Zhou J *et al.* Increased expression of EIF5A2, via hypoxia or gene amplification, contributes to metastasis and angiogenesis of esophageal squamous cell carcinoma. *Gastroenterology* 2014; **146**: 1701–1713.
22. Sato S, Itamochi H. Ovarian cancer and drug resistance. *Curr Obstet Gynecol Rep* 2015; **4**: 18–25.
23. Sato S, Itamochi H. Neoadjuvant chemotherapy in advanced ovarian cancer: latest results and place in therapy. *Ther Adv Med Oncol* 2014; **6**: 293–304.
24. Meads MB, Gatenby RA, Dalton WS. Environment-mediated drug resistance: a major contributor to minimal residual disease. *Nat Rev Cancer* 2009; **9**: 665–674.
25. Acker T, Plate KH. A role for hypoxia and hypoxia-inducible transcription factors in tumor physiology. *J Mol Med* 2002; **80**: 562–575.
26. Chen W, Wang C, Lin Y, Wu C, Hsieh C. Cycling hypoxia induces chemoresistance through the activation of reactive oxygen species-mediated B-cell lymphoma extra-long pathway in glioblastoma multiforme. *J Transl Med* 2015; **13**: 389.
27. Hubbia ME, Gilkesa DM, Hua H, Kshitizd, Ahmede I, Semenza GL. Cyclin-dependent kinases regulate lysosomal degradation of hypoxia-inducible factor 1α to promote cell-cycle progression. *PNAS* 2014: E3325–E3334.
28. Zhu Y, Zhao T, Itasaka S, Zeng L, Yeom C, Hirota K *et al.* Involvement of decreased hypoxia-inducible factor 1 activity and resultant G1–S cell cycle transition in radioresistance of perinecrotic tumor cells. *Oncogene* 2013; **32**: 2058–2068.
29. Le X, Bast RC. Src family kinases and paclitaxel sensitivity. *Cancer Biol Ther* 2011; **12**: 260–269.
30. Xu Q, Briggs J, Park S, Niu G, Kortylewski M, Zhang S *et al.* Targeting Stat3 blocks both HIF-1 and VEGF expression induced by multiple oncogenic growth signaling pathways. *Oncogene* 2005; **2005**: 5552–5560.
31. Niu G, Briggs J, Deng J, Ma Y, Lee H, Kortylewski M *et al.* Signal transducer and activator of transcription 3 is required for hypoxia-inducible factor-1α RNA expression in both tumor cells and tumor-associated myeloid cells. *Mol Cancer Res* 2008; **6**: 1099–1105.
32. Denisenkoa TV, Sorokinaa IV, Gogvadzea V, Zhivotovsky B. Mitotic catastrophe and cancer drug resistance: a link that must to bebroken. *Drug Resist Updat* 2015; **24**: 1–12.
33. Cypro P. The side effects of paclitaxel in solid tumors. *Eur J Cancer* 1996; **32**: S4.
34. Wu C, Yang C, Lee J, Hsu S, Tsai E. Weekly and monthly regimens of paclitaxel and carboplatin in the management of advanced ovarian cancer. A preliminary report on side effects. *Int J Gynecol Cancer* 2001; **11**: 295–299.
35. Hoensch H, Oertel R. The value of flavonoids for the human nutrition: short review and perspectives. *Clin Nutr Exp* 2015; **3**: 8–14.
36. Havsteen B. Flavonoids, a class of natural products of high pharmacological potency. *Biochem Pharmacol* 1983; **32**: 1141–1148.
37. Wang H, Zhao L, Zhu L, Wang Y, Pan D, Yao J *et al.* Wogonin reverses hypoxia resistance of human colon cancer HCT116 cells via downregulation of HIF-1 alpha and glycolysis, by inhibiting PI3K/Akt signaling pathway. *Mol Carcinog* 2014; **53**: E107–E118.

Supplementary Information accompanies this paper on Cell Death and Disease website (http://www.nature.com/cddis)